JOURNAL OF SOLID STATE CHEMISTRY 112, 58–64 (1994)

Hydroxyapatite Particles Synthesized by Pyrolysis of an Aerosol

M. Vallet-Regí,[1] M. T. Gutiérrez-Ríos, M. P. Alonso, M. I. de Frutos, and S. Nicolopoulos

Departamento de Química Inorgánica y Bioinorgánica, Facultad de Farmacia, Universidad Computense, 28040 Madrid, Spain

Received June 25, 1993; accepted October 25, 1993

Hydroxyapatite hollow particles have been prepared by pyrolysis of an aerosol produced by ultrahigh frequency of a $CaCl_2$–$(NH_4)H_2PO_4$ solution. Hollow particles were annealed at different temperatures. Thermal treatment at 1050°C produces the growth of nucleated crystallites in the particle surface, giving place to an spectacular morphology. The raspberry-shaped particles are polycrystalline, the crystallite size being controlled as a function of the annealing time. © 1994 Academic Press, Inc.

I. INTRODUCTION

Human calcified tissues (i.e., bones, teeth, and cartilages) are composed to a very large extent of hydroxyapatite (OHAp) crystals of chemical composition $Ca_{10}(PO_4)_6(OH)_2$ (1–3). Synthetic OHAp is a challengeable biomaterial for clinical applications (4–6). Physicochemical properties of this compound depend strongly on the crystal stoichiometry, i.e., on Ca/P ratio.

Although conceptually simple, the calcium phosphate system exhibits a rich and complex chemistry of solution and thermal treatments, which has been extensively studied in the past, but still continues to be the subject of intense research activity. This important proliferation of calcium phosphate based biomaterials with very different chemical compositions—not always reproducible—is a direct consequence of many factors such as the use of casual preparative techniques and the incomplete characterization of the final products.

Pure hydroxyapatite in powder form can be obtained and processed in many ways, in order to synthesize calcium phosphate based ceramics. In fact, very often the end products exhibit important compositional variations (i.e., relative percentage of hydroxyapatite phase and tricalcium phosphate), different morphology and texture, as well as variable porosity and grain size, resulting in an interesting way to distinguish mechanical properties and, consequently, medical applications.

A careful microstructural characterization of the hydroxyapatite compound is important in order to understand and to improve its properties and biocompatibility performances.

Possible applications and resistance to stress of the OHAp compound depend strongly on the initial synthesis, stoichiometry (ratio Ca/P) (5), sintering process (6), morphology (7, 8), crystallinity (9), and porosity (10).

As a consequence of the influence of numerous factors on physical properties (11) and possible biomedical applications (1, 11), it is of great importance to investigate the structural and morphological characteristics of the stoichiometric OHAp compound prepared in different ways.

Various techniques have been developed for the preparation of hydroxyapatites. More recently, the aerosol synthesis technique has been used to produce small particles of different materials (12, 13). Its main advantage is that this technique has the potential to create particles of unique composition, for which starting materials are mixed in a solution at atomic level. An ulterior thermal treatment can originate important modifications on morphology and texture. For these reasons it is interesting to prepare OHAp for this method.

We describe in this paper the synthesis of hydroxyapatite small particles by pyrolysis of an aerosol and the evolution of its microstructure after thermal treatment.

II. EXPERIMENTAL

Particle Preparation

Hydroxyapatite samples were synthesized by pyrolysis of an aerosol obtained from a precursor solution. To prepare this solution, analytical grade $CaCl_2 \cdot 2H_2O$ and $(NH_4)H_2PO_4$ (Merck) were used as starting reagents; 0.05 mol of $CaCl_2 \cdot 2H_2O$ was dissolved in 500 ml. of water and this solution was added in an aqueous solution of $(NH_4)H_2PO_4$ (0.06 *M*). The final pH of the solution was 5–6.

Hydroxyapatite fine particles were obtained by pyrolysis of an aerosol generated by ultrahigh frequency spraying of the solution previously prepared, according to the following experimental conditions: gas flow, 4.5 liters · min^{-1}; frequency, 850 KHz; carrier gas, pure air. A

[1] To whom correspondence should be addressed.

0022-4596/94 $6.00

full description of the processing equipment is given in Refs. (12, 13). An ultrasonic transducer is located at the bottom of a vessel containing a precursor solution of the final material. An ultrasonic beam is focused close to the surface of this solution. Ultrafine droplets (2–4 μm) are produced above the surface, and this aerosol is conveyed by air.

The aerosol flow passes through a 65-cm-long tubular furnace at a temperature of 500°C. Under these conditions, the residence time of particles is about 2 sec at high temperature. Thus, the solvent evaporates, leading to the formation of precursor particles and then submicronic hydroxyapatite particles.

Such particles are collected outside the furnace with an electrostatic filter. A thin tungsten wire is suspended in the center of a tubular stainless steel collection plate. This wire is negatively charged with 8 kV. The particles are then charged and collected on the plate which is kept at 150°C to avoid condensation of water steam. The collection efficiency is about 68%. The tungsten wire geometry avoids a powder accumulation on the fixing point of the wire and a short circuit of high voltage.

The *in situ* product so obtained, *OHAp* sample, was the object of several thermal treatments (see Table I) at different temperatures (500, 750, and 1050°C). The *in situ* material was annealed in the following way: two samples were heated in air at 500 and 750°C, respectively, for one hr. Other series of samples were placed in a furnace at 400°C and the temperature was raised by 5°C/min up to 1050°C. When this temperature was reached, different samples were collected after 10, 30, and 60 min, and 24 and 48 hr.

Particle Characterization

Chemical analysis of synthesized hydroxyapatite products was performed by atomic absorption analysis for calcium (Perkin–Elmer 2280) and by spectrophotometric nitromolybdatevanadate method for phosphorous.

Infrared spectroscopic measurements have been performed at room temperature using a Perkin—Elmer model 283 instrument, samples being prepared as KBr pellets.

Powder X-ray diffraction data were recorded on a Siemens D-5000 diffractometer using Cu$K\alpha$ radiation.

The particle morphology was examined by scanning electron microscopy (SEM) on a Jeol 6400 scanning electron microscope. Chemical analysis over some representative particles was carried out by Energy Dispersive Spectroscopy (EDS) on a Link AN 10000 system.

The samples for TEM observations were ultrasonically dispersed in *n*-butanol and then transferred to carbon-coated copper grids. The examination was performed on a JEOL 2000 FX electron microscope equipped with a double tilt specimen stage.

III. RESULTS AND DISCUSSION

Chemical analysis of Ca and P content of the *in situ* obtained material as well as in the annealed hydroxyapatite samples revealed that the molar ratio is Ca/P = 1.667 $\pm$ 0.005, in agreement with the stoichiometric hydroxyapatite formula

Infrared (IR) spectra performed on different samples (Fig. 1) show the typical absorption bands of hydroxyapatite. All examined samples reveal two characteristic absorption bands, at 1090–1050 cm^{-1}, corresponding to the antisymmetric stretching vibration mode of the phosphate group. A single absorption band at 960 cm^{-1} can be assigned to the symmetric vibration mode, and the two bands at 600 and 570 cm^{-1} correspond to the bending mode of the phosphate group (14, 15).

A wide band at 3400 cm^{-1} corresponding to H_2O, appears in the following samples: OHAp *in situ*, $A_{60\ min}$, $B_{60\ min}$, $C_{10\ min}$, $C_{30\ min}$, and $C_{60\ min}$. At the same time, no absorption bands corresponding to the OH group of the hydroxyapatite are observed. Two absorption bands at 3570 cm^{-1} (stretching mode) and 630 cm^{-1} (bending mode), corresponding to the OH group, appear in the $C_{24\ hr}$ and $C_{48\ hr}$ samples. This fact proves the good crystallinity of the above-examined samples (15–17).

Powder XRD patterns corresponding to *in situ* and to the thermally treated samples, are observed in Fig. 2. Synthesized OHAp shows the presence of a broad amorphous background in the X-ray diffraction patterns, but sintering of the samples leads to a better crystallinity which can be revealed from the very sharp diffraction peaks. Amorphous background in the X-ray diffraction patterns disappears after thermal treatment at a temperature of 1050°C for 24 hr.

TABLE 1
Denomination of Both *in Situ* and Annealed Materials

	Annealed samples						
In situ sample	500°C/1 hr	750°C/1 hr	1050°C/10 min	1050°C/30 min	1050°C/60 min	1050°C/24 hr	1050°C/48 hr
$OHAp_{in\ situ}$	$A_{60\ min}$	$B_{60\ min}$	$C_{10\ min}$	$C_{30\ min}$	$C_{60\ min}$	$C_{24\ hr}$	$C_{48\ hr}$

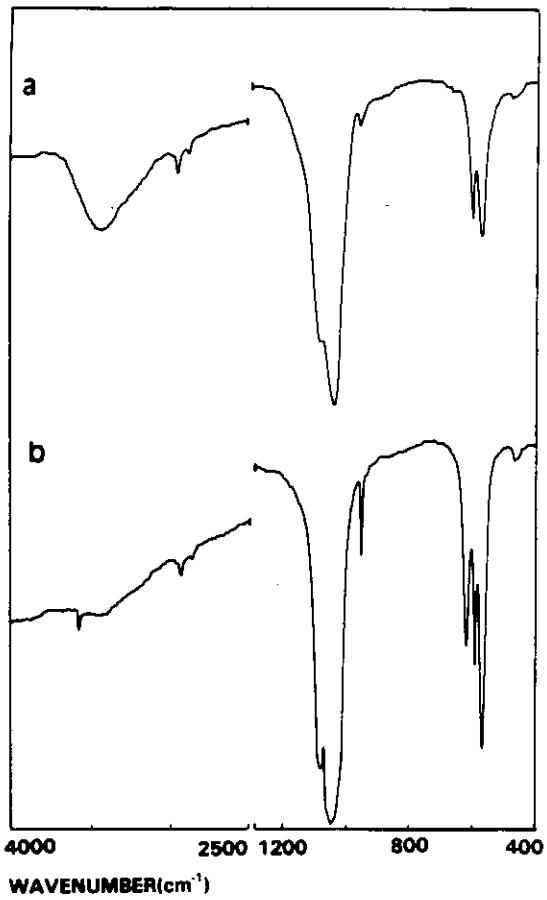

FIG. 1. IR spectra of the samples (a) *in situ* OHAp and (b) $C_{24\ hr}$.

All thermally treated samples can be indexed in a unique way as hydroxyapatite although crystal lattice parameters vary depending on the type of the thermal treatment. Table 2 summarizes the lattice constants of products annealed at different thermal conditions. In accordance with Brendel *et al.* (18) we effectively observe an increase of the c_0 parameter (and at the same time a decrease of the a_0 parameter) at higher sintering temperatures. We also observe that for T = 1050 °C such a variation is also a function of the time. The change observed in the unit cell

TABLE 2

Lattice Constants a_0 and c_0 of Hydroxyapatite Samples (SG $P6_3/m$) Annealed at Different Temperatures

Samples	Lattice constants (nm)	
	a_0	c_0
$OHAp_{in\ situ}$	0.959	0.679
$B_{60\ min}$	0.954	0.680
$C_{10\ min}$	0.952	0.683
$C_{24\ hr}$	0.940	0.686

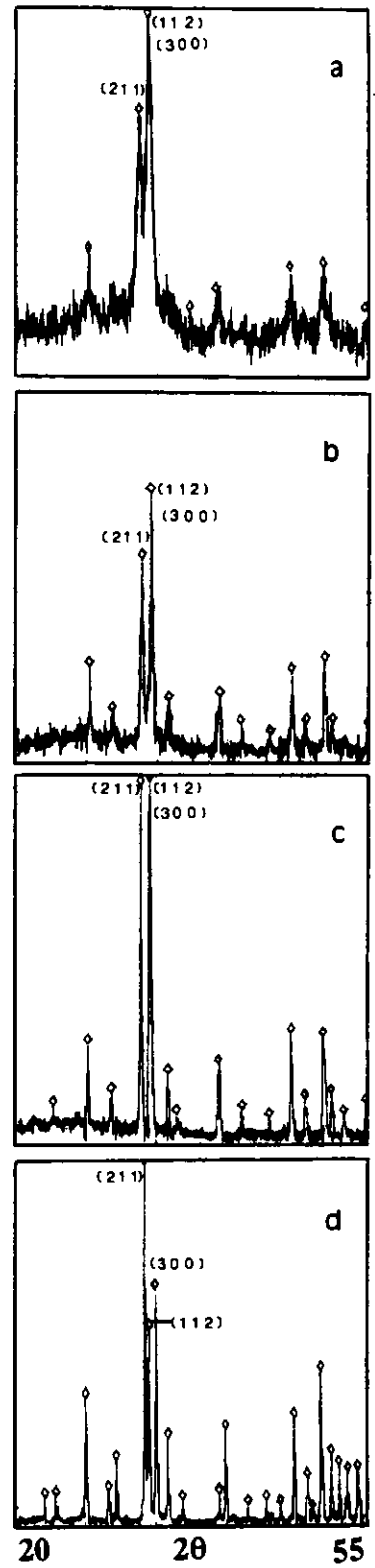

FIG. 2. Powder XRD patterns of the samples (a) *in situ* OHAp, (b) $B_{60\ min}$, (c) $C_{10\ min}$, and (d) $C_{24\ hr}$.

parameters practically ends when the amorphous background disappears. This is probably a suggestion of a compositional change of the crystalline phase which is being fed by the remnant amorphous phase.

The above sintered apatite powders show the following crystallographic characteristic: in the *in situ* $B_{60\ min}$, and $C_{10\ min}$ samples (112) and (300) reflections overlap; at $C_{24\ hr}$ sample, the latter reflections are clearly distinguished. This fact is in accordance with the results of previous work (19).

It should be mentioned that impurity phases such as tricalcium phosphate, tetracalcium phosphate, or calcium oxide have not been observed.

All hydroxyapatite samples have been analyzed by EDS in order to detect the possible presence of chlorine due to the NH_4Cl formation during the pyrolysis process. On every hydroxyapatite thermally treated below 1000°C, or at 1050°C during short periods of time (no more than 60 min), the presence of chlorine can be clearly detected. The chlorine amount on these samples proportionally decreases by increasing both the sintering temperature and the annealing time. In fact, in the $C_{30\ min}$ and $C_{60\ min}$ samples only very small amounts of chlorine are present, and in $C_{24\ hr}$ and $C_{48\ hr}$ samples no chlorine could be detected.

All prepared samples were analyzed by SEM in order to observe the morphological evolution as a function of the thermal treatment. In the *in situ* prepared OHAp sample hollow particles of mean size 1.2 μm can be observed (Fig. 3), which are approximately spherical but have different crystal morphologies and the same chemical composition, according to EDS analysis.

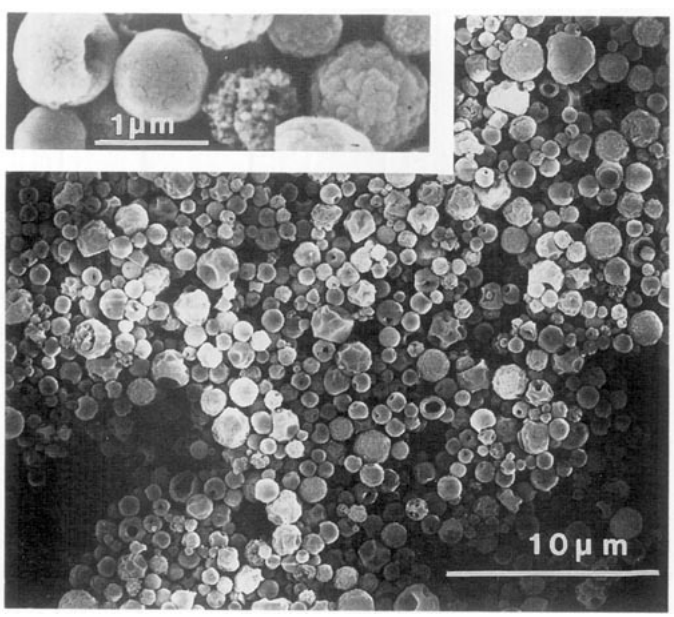

FIG. 3. Scanning electron micrograph of the *in situ* OHAp sample. An enlargement is seen in the inset.

All the thermal treatments at temperatures below 1050°C have no influence neither on particle size, nor on chemical composition, as long as the molar ratio Ca/P remains the same as observed from EDS analysis.

In fact, when samples are thermally treated at temperatures below 1000 °C, every large hollow particle contains a hundred smaller crystallites. This is confirmed by electron diffraction analysis performed on several individual hollow particles; as seen in Fig. 4a which corresponds to a typical polycrystalline material.

On the other hand, thermal treatments at 1050°C may induce changes in crystallite size and morphology of the particle depending on the duration of the cumulative thermal treatment. In fact, for 10 min sintering at 1050°C particles appear having a raspberry-like morphology, constituted by a hundred small crystallites. The particles are still hollow, but the nucleated crystallites grow up in their surface giving place to that capricious raspberry-like shape (Fig. 5). For 30 and 60 min sintering, the particle's size remains approximately constant, with a mean value of 1.2 μm. At the same time, the raspberry-like morphology is even more accentuated (Fig. 6). As a consequence of the inhomogeneity of the particle size distribution, we can detect some particles as small as 0.3 μm and as large as 2.2 μm. In any case, the size more frequently found is 1.2 μm. On the other hand, independent of the temperature used in the annealed process, the size of each single particle is constant and crystallites form on its surface. This growth increases when the temperature is higher and the annealing process is longer.

When the sintering temperature is higher (1050°C) better crystallinity and a considerable increase of the crystallite size grown on each individual hollow particle is observed by X-ray diffraction. Nevertheless, at this sintering temperature, the treatment time is of particular importance: for sintering times equal at 60 min, the material is well crystallized, as is effectively observed from X-ray data. Moreover, electron diffraction of individual hollow particles show typical patterns of several superimposed monocrystalline materials (Fig. 4b).

On the other hand, for sintering times lower than 60 min small crystallites have an intermediate size in comparison with those grown during the thermal treatment below 1000°C and those grown during the treatment at 1050°C for 60 min; the diffraction pattern sometimes exhibits an aspect of a typical polycrystalline material and sometimes has the aspect of several superimposed monocrystalline particles (Fig. 4c).

Nevertheless, for longer thermal treatments at 1050°C (24 and 48 hr) sintering of the particles leads to the formation of crystal aggregates as a consequence of the fusion between individual particles (Fig. 7). Those aggregates show rounded boundaries with large sized pores between them.

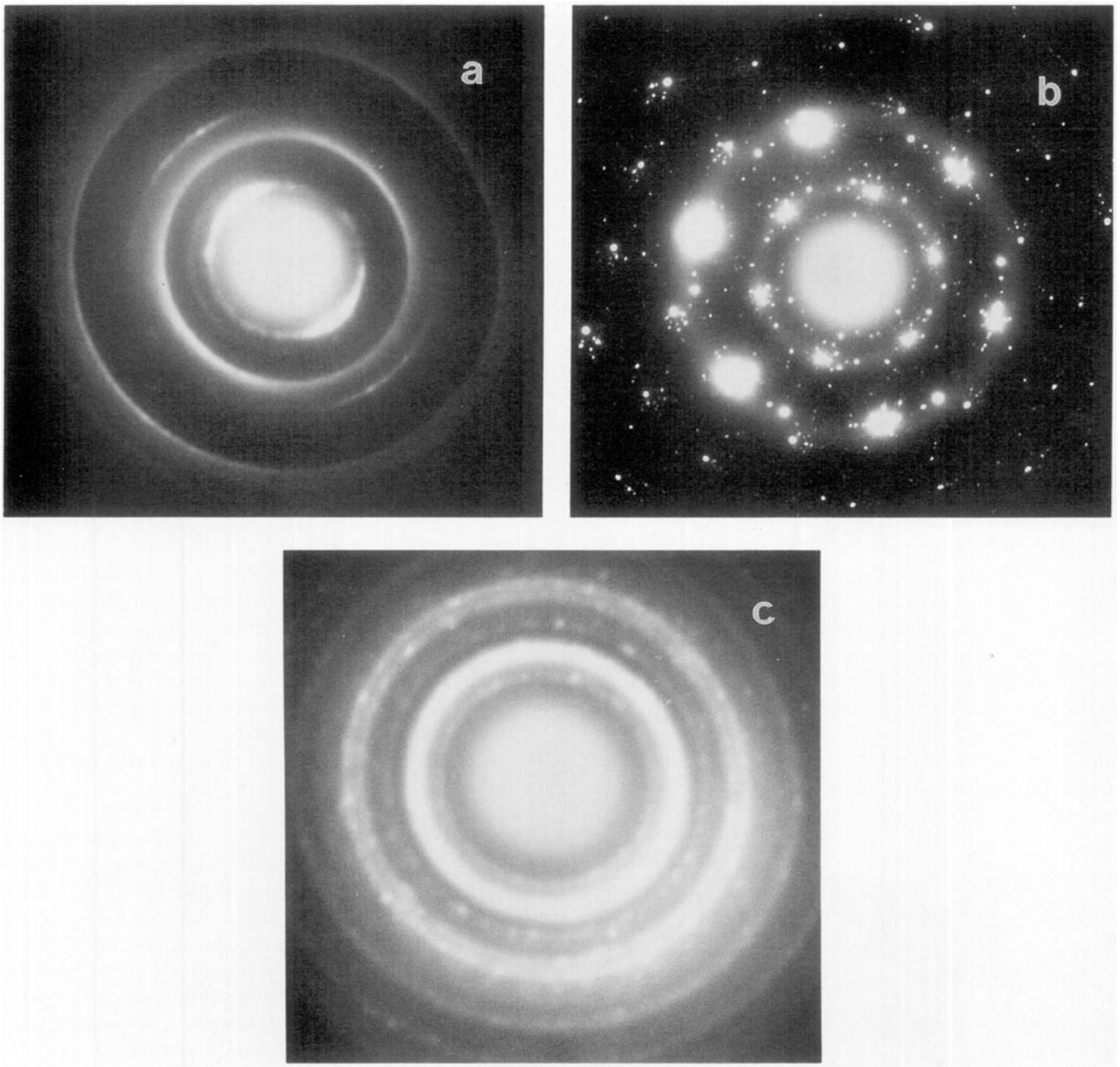

FIG. 4. Electron diffraction patterns of the hydroxyapatite samples (a) $A_{60\ min}$, (b) $C_{60\ min}$, and (c) $C_{10\ min}$.

IV. CONCLUSIONS

The synthesis of hydroxyapatite by pyrolysis of an aerosol leads to small hollow particles. The ulterior thermal treatment modified both the particle shape and the size of crystallites. The initial spherical shape evolutes to a raspberry-like shape at a temperature of 1050°C. The mean size particle is 1.2 μm, but as a consequence of the inhomogeneity of the particle size, a range of particle size between 0.3 and 2.2 μm is detected. The particles are formed by small crystallites whose size could be controlled as a function of the annealing time.

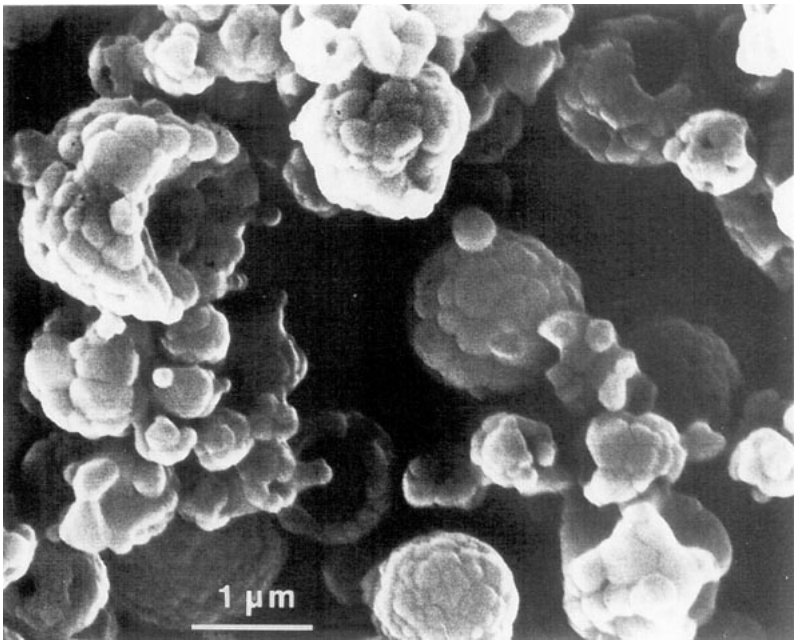

FIG. 5. Scanning electron micrograph of the $C_{10\ min}$ sample.

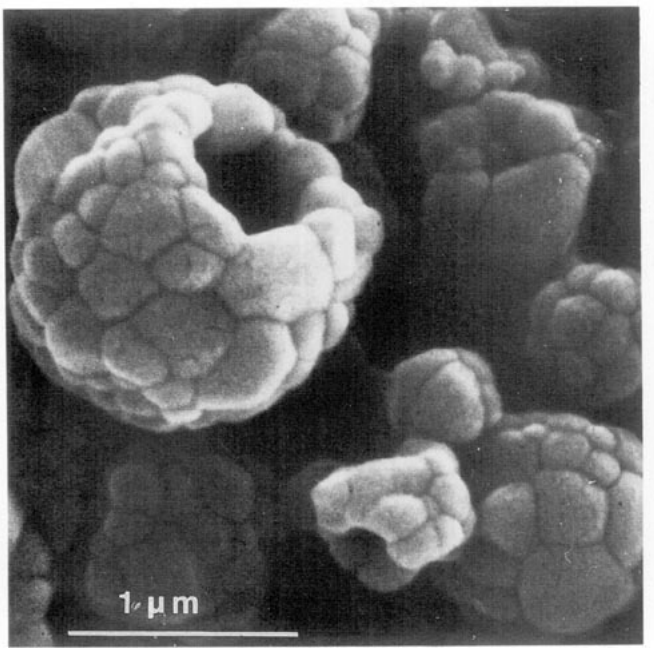

FIG. 6. Scanning electron micrograph of the $C_{30\ min}$ sample.

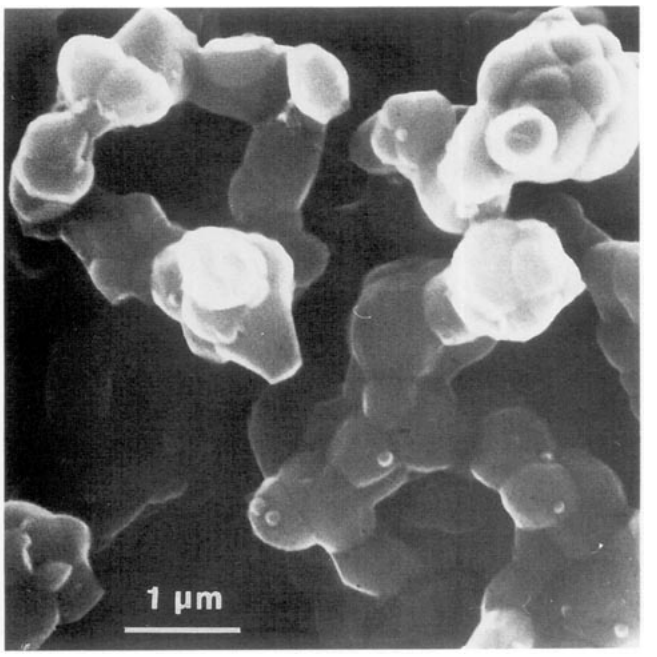

FIG. 7. Scanning electron micrograph of the $C_{48\ hr}$ sample.

ACKNOWLEDGMENTS

We thank Professor J. M. González-Calbet for a full discussion of the paper. We acknowledge the financial support of CICYT (Spain) through Research Project MAT 93-0207. We also thank Dr. J. L. Martínez Fernández-Ballesteros for valuable discussions, and J. L. Baldomero and A. Rodriguez for technical assistance.

REFERENCES

1. L. L. Hench and J. Wilson, *M.R.S. Bull. XVI* **9,** 62 (1991).
2. K. de Good, R. Geesink, C. P. A. T. Klein, and P. Serekian, *J. Biomed. Mater. Res.* **21,** 1375 (1987).
3. H. Solnick-Legg and K. Legg, *M.R.S. Bull.* **14,** 27 (1989).
4. N. M. Meenen, J. F. Osborn, M. Dallek, and K. Donath, *J. Mater. Sci.: Mater. in Med.* **3,** 345, (1992).
5. A. Royer, J. C. Viguie, M. Heughebaert, and J. C. Heughebaert, *J. Mater. Sci.: Mater. in Med.* **4,** 76, (1993).
6. W. Bohne, J. A. Pouezat, and G. Daculsi, *in* "Proceedings, Fourth World Biomaterials Congress, Berlin," p. 1, 1992.
7. V. F. Komarov and I. V. Melikhov, *in* "Proceedings, Fourth World Biomaterials Congress, Berlin," p. 320, 1992.
8. F. Lelièvre and D. Bernache-Assollant, *in* "Proceedings, Fourth World Biomaterials Congress, Berlin," p. 330, 1992.
9. C. Gabbi, P. Borghetti, A. Cachioli, N. Antolotti, and S. Pitteri, *in* "Proceedings, Fourth World Biomaterials Congress," Berlin p. 5, 1992.
10. Yi Fang, D. K. Agrawal, Della M. Roy, and R. Roy, *J. Mater. Res.* **7**(2), 490 (1992).
11. M. N. Helmus, *M.R.S. Bull. XVI* **9,** 33 (1991).
12. M. V. Cabañas, J. M. González-Calbet, M. Labeau, P. Mollard, M. Pernet, and M. Vallet-Regí, *J. Solid State Chem.* **101,** 265 (1992).
13. M. Vallet-Regí, V. Ragel, J. Román, J. L. Martínez, M. Labeau, and J. M. González-Calbet, *J. Mater. Res.* **8**(1), 138 (1993).
14. E. E. Berry, *J. Inorg. Nucl. Chem.* **29,** 317 (1967).
15. S. R. Radin, P. Ducheyne, *J. Mater. Sci.: Mater. in Med.* **3,** 33 (1992).
16. J. Zhon, X. Zhang, J. Chen, S. Zeng, and K. de Groot, *J. Mater. in Med.* **4,** 83 (1993).
17. Venkata S. Nagarajan and Kalya J. Rao, *J. Mater. Chem.* **3**(1), 43 (1993).
18. T. Brendel, A. Engel, and C. Rüssel, *J. Mater. Sci.: Mater. in Med.* **3,** 175 (1992).
19. T. Hattori, Y. Iwadate, and T. Kato, *J. Mater. Sci. Lett.* **8,** 305 (1989).